Proc. Natl. Acad. Sci. USA
Vol. 90, pp. 6503–6507, July 1993
Cell Biology

Single kinesin molecules crossbridge microtubules *in vitro*

(scanning transmission electron microscopy/molecular structure/cytoskeleton)

S. B. ANDREWS*, P. E. GALLANT*, R. D. LEAPMAN†, B. J. SCHNAPP‡, AND T. S. REESE*§

*Laboratory of Neurobiology, National Institute of Neurological Disorders and Stroke; †Biomedical Engineering and Instrumentation Program, National Center for Research Resources, National Institutes of Health, Bethesda, MD 20892; and ‡Department of Cellular and Molecular Physiology, Harvard Medical School, Boston, MA 02115

Contributed by T. S. Reese, February 22, 1993

ABSTRACT **Kinesin is a cytoplasmic motor protein that moves along microtubules and can induce microtubule bundling and sliding *in vitro*. To determine how kinesin mediates microtubule interactions, we determined the shapes and mass distributions of squid brain kinesin, taxol-stabilized microtubules (squid and bovine), and adenosine 5′-[β,γ-imido]triphosphate-stabilized kinesin–microtubule complexes by high-resolution metal replication and by low-temperature, low-dose dark-field scanning transmission electron microscopy of unfixed, directly frozen preparations. Mass mapping by electron microscopy revealed kinesins loosely attached to the carbon support as asymmetrical dumbbell-shaped molecules, 40–52 nm long, with a mass of 379 ± 15 kDa. The mass distribution and shape of these molecules suggest that these images represent kinesin in a shortened conformation. Kinesin–microtubule complexes were organized as bundles of linearly arrayed microtubules, stitched together at irregular intervals by crossbridges typically ≤25 nm long. The crossbridges had a mass of 360 ± 15 kDa, consistent with one kinesin per crossbridge. These results suggest that kinesin has a second microtubule binding site in addition to the known site on the motor domain of the heavy chain; this second site may be located near the C terminus of the heavy chains or on the associated light chains. Thus, kinesin could play a role in either crosslinking or sliding microtubules.**

The kinesins are a family of cytoplasmic motors whose members are readily extracted from many types of cells (1, 2). The motor function of kinesin was originally defined by the ability of squid brain kinesin, in the presence of ATP, to promote movements of latex beads and other negatively charged surfaces toward the plus ends of microtubules (2). Subsequently, biochemical, molecular, and structural characterization of kinesin molecules from different sources showed that these motor proteins are elongated molecules with distinct globular ends (3, 4). It is now known that the bilobed end—the motor end (5, 6)—consists of the N-terminal region of paired heavy chains (3), each containing a microtubule binding site and a consensus sequence for ATPase activity (5, 7–9). The motor end couples ATP hydrolysis to movement along microtubules (6), whereas the other end is thought to bind kinesin to organelles or to other substrates moved by kinesin.

It is now widely accepted that kinesin is the motor involved in anterograde transport of organelles in the axons of nerve cells, where microtubules are oriented with their plus ends distal (10). Evidence that kinesin can indeed move organelles *in situ* comes from blocking movements of organelles by injecting antibodies against heavy chain into the squid giant axon (11). Another approach, reconstituting the movements of highly purified organelles along microtubules, has succeeded in reproducing the native rate and direction of movement (12). In these experiments, however, addition of soluble kinesin was not necessary because organelle-bound kinesin was carried through the purification. Since this tightly associated kinesin is sufficient to produce the organelle movements, there may be other roles for the large pool of cytoplasmic kinesin (2).

It has recently been shown that adding kinesin to suspensions of microtubules can lead to bundling as well as to translocation of microtubules along other microtubules (13). These experiments suggest that kinesin could also have a role in microtubule–microtubule interactions, which might be mediated by a second microtubule binding site on a single kinesin molecule—either the recently described site on the C terminus of heavy chains (14) or a site on the light chains themselves. It remains possible, however, that homopolymers of kinesin could crosslink microtubules and promote microtubule sliding while attaching exclusively by ATP-sensitive binding sites on the motor end. To choose between these possibilities, it was necessary to directly visualize how kinesin molecules associate with bundles of microtubules.

It has, in general, been difficult to use electron microscopy to characterize the structure of kinesin or other microtubule-associated proteins while they are attached to microtubules; methods that depend on fixation frequently distort the assemblies (15), whereas unfixed, unstained preparations are fragile and low in contrast (16). Therefore, it was necessary to use a new technique (17), based on rapid freezing of thin films (18), to prepare kinesin–microtubule complexes for parallel high-resolution metal replication and low-dose, dark-field scanning transmission electron microscopy (STEM) (19). With these techniques, single kinesin molecules attached to microtubules could be visualized and identified by their shape, molecular mass, and mass distribution. The results show that the light-chain end as well as the heavy-chain end of individual kinesin molecules can bind to microtubules, leading to the formation of stable crossbridges consisting of single kinesin molecules.

MATERIALS AND METHODS

Purification of Microtubules and Kinesin. Microtubules were purified from squid optic lobe essentially as described (12, 20), except that polymerization of microtubules was carried out at 17°C. Phosphocellulose-purified bovine tubulin was used in a few experiments, with results that did not differ from those with squid tubulin. Kinesin was purified (12, 20) using motility buffer (12) in place of BRB80 buffer.

Preparation of Microtubule–Kinesin Complexes. Microtubule–kinesin complexes were formed by combining ≈1 μM purified kinesin with ≈10 μM microtubule-associated protein

The publication costs of this article were defrayed in part by page charge payment. This article must therefore be hereby marked "*advertisement*" in accordance with 18 U.S.C. §1734 solely to indicate this fact.

Abbreviations: STEM, scanning transmission electron microscopy; AMP-PNP, adenosine 5′-[β,γ-imido]triphosphate; MAP, microtubule-associated protein.

§To whom reprint requests should be addressed at: Building 36, Room 2A-29, National Institutes of Health, Bethesda, MD 20892.

(MAP)-free microtubules in the presence of 5–10 mM adenosine 5′-[β,γ-imido]triphosphate (AMP-PNP) and 20 μM taxol in motility buffer at room temperature for 30–60 min. The complexes were spun in a Beckman Airfuge for 30–60 min at 150,000 × *g*. Pellets were resuspended in taxol-containing motility buffer prior to adsorption to specimen supports. In some instances, complexes were broken up by triturating a 50- to 100-μl sample 100 times through a 50-μl plastic pipette tip.

Sample Preparation for Electron Microscopy. Specimen supports were prepared by evaporating ≈3 nm of carbon onto freshly cleaved mica (17). The carbon film was floated on deionized water and applied to 600-mesh grids coated with holey Formvar nets; the film was then rinsed in buffer and kept continuously wet throughout processing. Proteins were adsorbed by injecting samples under the grid and incubating for 1–2 min (19). Grids were rinsed twice each in taxol-containing motility buffer and 150 mM ammonium acetate, blotted to a thin film with filter paper, and frozen in a liquid nitrogen-cooled mixture of ethane/propane. Parallel samples were negatively stained with 1% uranyl acetate.

Electron Microscopy. Frozen specimens were cryotransferred into a Balzers 301 freeze-etch device, freeze-dried for 4 h while warming to −40°C, rotary shadowed (15° angle) at −110°C with Pt/Ir/C followed by vertical shadowing with ≈3 nm of carbon, and examined directly in a JEOL 200CX electron microscope (17). The mass of freeze-dried protein complexes was determined by low-dose, dark-field STEM (19). STEM images were recorded with single-electron sensitivity in a VG Microscopes (East Grinstead, U.K.) HB501 STEM operating at 100 kV and equipped with a cryotransfer stage and cold-field emission source (21). Data were typically acquired as 512 × 512 pixel images at approximately −160°C, ≈5 pA probe current, 0.9- to 1.8-nm pixel size (<1 nm probe size), and 100-μs dwell time, resulting in doses of 800–3000 electrons per nm^2. Images were analyzed on Apple Macintosh II series computers using the image processing program IMAGE (available from W. S. Rasband, National Institute of Mental Health, National Institutes of Health).

RESULTS

Kinesin Mediates Microtubule Bundling. Reassembled, taxol-stabilized microtubules, essentially free of MAPs, were prepared from squid or bovine brain tubulin. Microtubules at suitable concentrations (as determined by negative-stain electron microscopy) were adsorbed to hydrophilic carbon support films, frozen as thin films, and examined by high-resolution platinum replication and by low-dose, low-temperature dark-field STEM (19). The former provides stereoviews of microtubule assemblies down to the level of tubulin subunits (17), whereas the latter gives a direct measure of the molecular mass of unfixed biological specimens (19, 21). Typical MAP-free microtubules, many micrometers long and with smooth, clean edges, had a mass per unit length of 176 kDa/nm (Table 1), which compares favorably with the 178 kDa/nm expected for MAP-free, 13-protofilament microtubules.¶ Microtubules ordinarily showed no tendency to self-associate, but when incubated in the presence of purified squid brain kinesin and the nonhydrolyzable ATP analog AMP-PNP, they associated into large clumps. These clumps consisted of bundles of many parallel or antiparallel microtubules, which frequently splayed out into smaller bundles (Fig. 1). The formation of bundles was dependent on the presence of kinesin (2, 13).

Table 1. Molecular masses of squid brain kinesin, microtubules, and kinesin–microtubule assemblies

Molecules	Molecular mass, kDa
Taxol-stabilized microtubules	176 ± 2*
Free kinesin	
Complete molecules	379 ± 15 (33)
Segments of complete molecules†	
Larger domain	194 ± 22 (7)
Stalk domain	52 ± 27 (7)
Smaller domain	123 ± 14 (7)
Incomplete molecules‡	214 ± 14 (15)
Microtubule-associated kinesin	
Complete molecules, bridging	360 ± 15 (17)
Complete molecules, sidearm§	384 ± 23 (16)
Incomplete molecules, sidearm§	228 ± 9 (15)

Data are the mean ± SEM; the number of analyzed molecules is given in parentheses.
*Mass per unit length in kDa/nm. The total length of analyzed structures was 4200 nm.
†Kinesin molecules were segmented into three regions, as defined in Fig. 3. The summed molecular mass of the segments is 369 kDa.
‡Globular structures, ≈14 nm in diameter. This is the only major subset with a molecular mass less than that of single kinesin molecules.
§Defined as clear projections from the edge of one microtubule where interaction with a second microtubule was not possible.

Examination of replicas revealed that the parallel microtubules of the kinesin-containing bundles were stitched together by frequent, irregularly spaced crossbridges (Fig. 2*a*); such bridges were never found in the absence of kinesin, even at places where microtubules crossed. Where microtubules lay directly on the support, the crossbridges appeared to dictate a microtubule–microtubule spacing of ≈25 nm. Some crossbridges had the characteristic size and bilobed appearance of single kinesin molecules (Fig. 2*a Inset*) (3). However, we could not be sure that these were single kinesins on the basis of structural criteria alone, since support film adsorption tends to distort molecules (23) while metal replication increases their size.

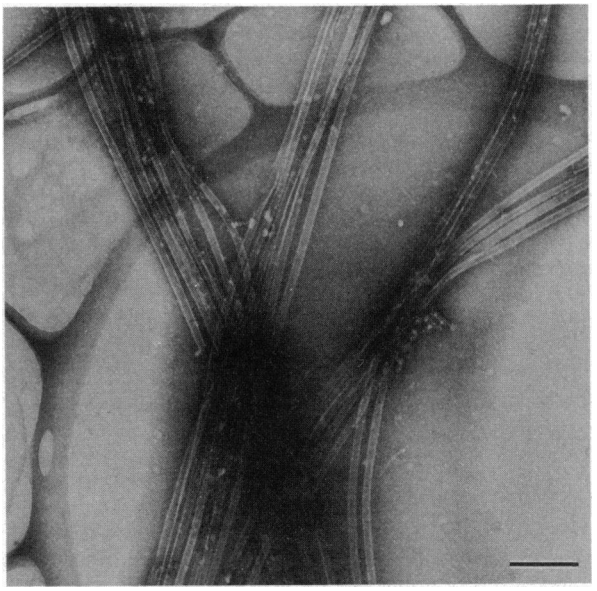

FIG. 1. Negative-stained microtubule–kinesin complexes bundled in the presence of kinesin and AMP-PNP and adsorbed to carbon film supported on a holey Formvar net. This is the type of preparation used for STEM. (Bar = 200 nm.)

¶This calculation assumes a molecular mass of 110 kDa for α/β tubulin and ignores posttranslational modifications. A previous STEM study of microtubules gave a mass per unit length of 210 ± 19 kDa/nm, but, as the authors pointed out, a significant complement of MAPs was present (22).

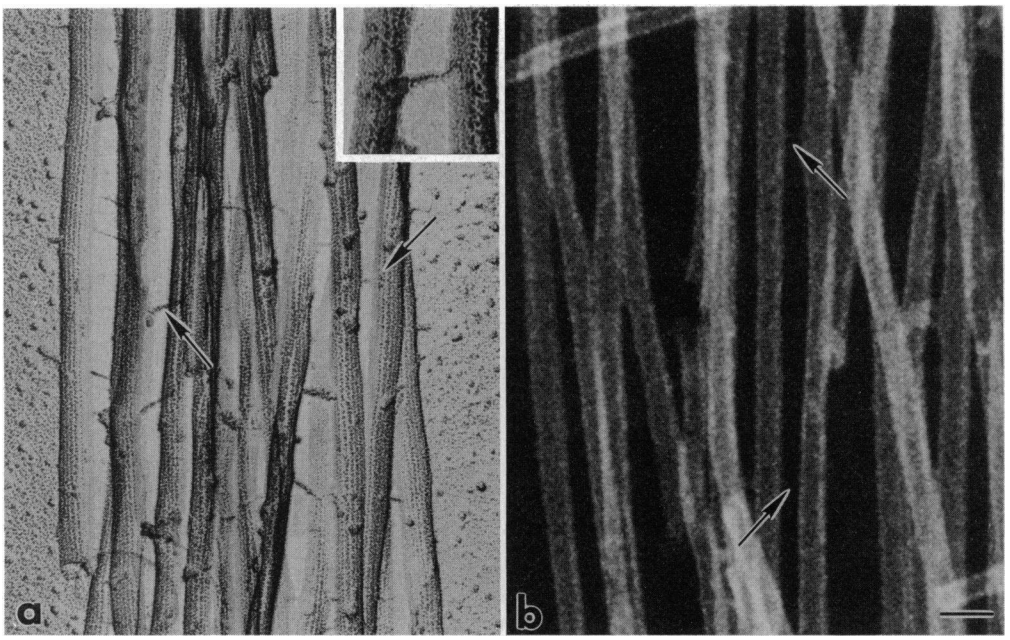

FIG. 2. Microtubule–kinesin complexes directly frozen as thin films. (*a*) Platinum alloy replica of freeze-dried thin film reveals numerous crossbridges between microtubules. Variations in density and thickness are attributed to differences in accessibility of the bridge to rotary-shadowed alloy. (*Inset*) Crossbridge showing a large end (left) and a small end (right), a shape compatible with that of kinesin. (*b*) Similar field as seen by low-dose dark-field STEM. Arrows indicate comparable crossbridges, which are numerous but difficult to see at this magnification and contrast (compare with Fig. 4). Even when visible, crossbridges appear thinner than in *a* because they have not been shadowed. Both marked crossbridges have molecular masses compatible with single kinesins. (Bar = 50 nm.)

Directly frozen preparations of microtubule–kinesin assemblies were also imaged in the STEM (21). Following cryotransfer and freeze-drying, digital micrographs were recorded in the elastic dark-field mode at approximately −170°C. Such images, in which the intensity is proportional to the mass, constitute mass maps of the specimen (19). Dark-field STEM images of microtubule–kinesin assemblies were quite comparable to replicas, including the presence of crossbridges (Fig. 2*b*). The bridges were unambiguous, even though they were difficult to find in dark-field images, in large part because their molecular mass is low relative to that of the attached microtubules.

Shape and Molecular Mass Distribution of Isolated Kinesin. Kinesin has not previously been characterized by direct observation of native molecules. Therefore, STEM images of single kinesins were recorded from molecules adsorbed onto carbon from solutions of purified kinesin or selected from microtubule-free regions of microtubule/kinesin preparations. Images of kinesins from these two types of preparations did not differ significantly (Figs. 3 and 4*a*). The structure of isolated kinesin molecules was dependent on the surface properties of the carbon film to which they were adsorbed. Kinesin molecules adsorbed to the moderately hydrophilic carbon films used here—films that maintain microtubules as hollow cylinders 23–25 nm in diameter (17)—appeared as asymmetrical, dumbbell-shaped structures with an average molecular mass of 379 kDa (Fig. 3 and Table 1), but a length of only 40–56 nm. In contrast, kinesin molecules adsorbed to more adhesive films appeared as rod-like molecules, ≥60 nm long, with bulbous ends. Images of this extended form of kinesin (not shown) were comparable to those previously described (3, 4, 15, 24).

In favorable orientations, these shorter kinesins could be divided into morphological domains (Fig. 3). Analysis of mass distribution between domains leads to the conclusion that the end of higher molecular mass is, in fact, the light-chain end of the molecule. The thin central stalk was typically 24 nm long with a mass (52 kDa) consistent with a coiled-coil α-helix of this length (Table 1). This piece could account for about half, but not all, of the α-helical rod domains (rod I and rod II) of paired squid kinesin heavy chains (9). To reconcile the STEM data with existing models of kinesin structure (3–5, 7, 9), we postulate that most of the paired rod II segment (≈40 kDa) is not part of the visible stalk but is included within the larger light-chain domain. The data (Fig. 3 and Table 1) fit well with this model, which gives a predicted molecular mass distribution of 206 kDa and 92 kDa for the heavier and lighter ends, respectively (9). The data, however, are also statistically compatible with an arrangement in which 40 kDa of the rod I helices are incorporated into the globular motor end. The former arrangement is more attractive, in that it avoids folding the stiffer rod I helix, while placing the putative hinge region [amino acid residues 560–580 (9)] near the boundary between the stalk and the larger end. Globular subfragments with a molecular mass similar to that of two heavy chains were also frequently observed (Table 1); these fragments remain uncharacterized.

Single Kinesin Molecules Can Crossbridge Microtubules. Once the shape and mass distribution for single kinesins were known, it was possible to determine whether the bridges and sidearms decorating bundled microtubules were also kinesin molecules. In fact, the bridging molecules were structurally similar to single kinesins, once allowance was made for overlap with the microtubules (Fig. 2; compare *a* and *b* in Fig. 4). Moreover, the molecular mass of the bridging structures,

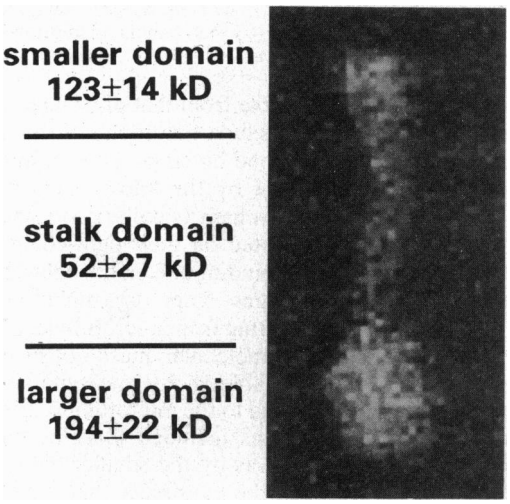

FIG. 3. Dark-field STEM of a single representative kinesin molecule attached to a carbon substrate. The digitally filtered dark-field image reveals a bilobed structure from which boundaries of structural domains can be estimated. This kinesin molecule is 52 nm long. Resolution = 0.9 nm per pixel.

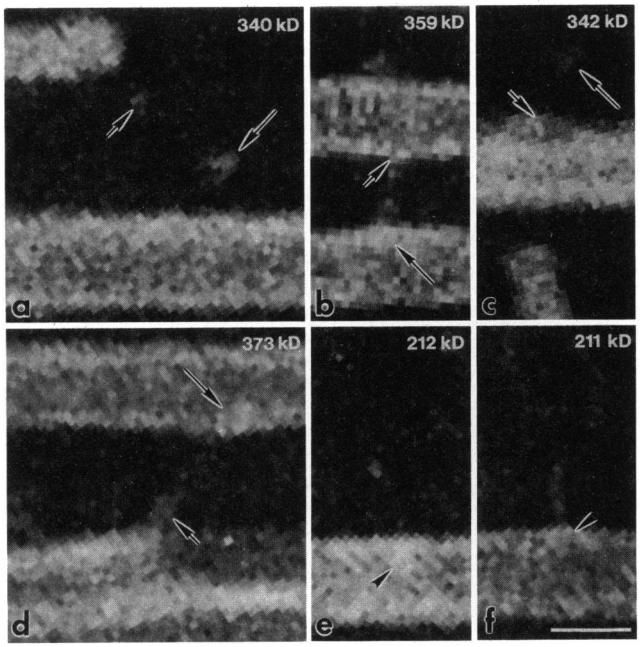

FIG. 4. Gallery of representative dark-field STEM micrographs of kinesin–microtubule complexes. Each example illustrates structural features of a different kinesin moiety that define a mass analysis group; quantitative results (Table 1) are averages from several equivalent images within each group. The molecular mass for specific kinesin moieties shown is given on each panel. Long arrows point to larger ends of kinesin molecules while short arrows point to smaller ends. (*a–c*) Standard preparation. (*a*) Kinesin molecule attached only to substrate. Segments of microtubule (below) and tobacco mosaic virus [above left, for mass calibration (19)] are also shown. (*b*) Kinesin molecule bridging a pair of microtubules. The bridge length is 22 nm. (*c*) Complete kinesin molecule attached to one of two overlapping microtubules by its smaller end; a second, almost parallel microtubule crosses the first one near the attachment. A segment of tobacco mosaic virus is below. (*d–f*) Triturated microtubule–kinesin complexes. (*d*) Kinesin in extended form still bridging two microtubules. The bridge length is 36 nm. The lower microtubule has been torn open to the right of the bridge. (*e* and *f*) Putative kinesin-related sidearms (arrowheads) attached by only one end with molecular masses significantly lower than complete molecules. The sidearm in *e* could plausibly be paired kinesin heavy chains only (expected molecular mass of 220–250 kDa), in which case the absence of light chains and the length of stalk (30 nm) imply attachment by the motor end. (*f*) The stalk is 21 nm long, leaving the nature of this sidearm uncertain. (For all panels, resolution = 1.8 nm per pixel; bar = 25 nm.)

360 kDa, was indistinguishable from that of isolated kinesins (Table 1). We therefore conclude that many of the microtubule crossbridges were formed by single kinesin molecules, attached to one microtubule by the known motor domain binding site on their heavy-chain (smaller) end and to the other by a binding site located on their light-chain (larger) end. Further evidence for a binding site on the light-chain end of the kinesin complex came from dark-field images of nonbridging sidearms projecting from microtubules. Many of these sidearms also had a molecular mass consistent with single, complete kinesins (Table 1). By mass analysis of the globular segment not attached to the microtubule surface, we determined that the sidearms included kinesins bound by both the larger ends as well as by the smaller ends.

These results leave open the possibility that the observed light-chain end binding is artifactual, adventitious, or weak. Therefore, specimens were prepared in which the bundles were mechanically disrupted before adsorbing them to the carbon support. In such preparations the microtubule bundles appeared stretched and torn, and it was straightforward

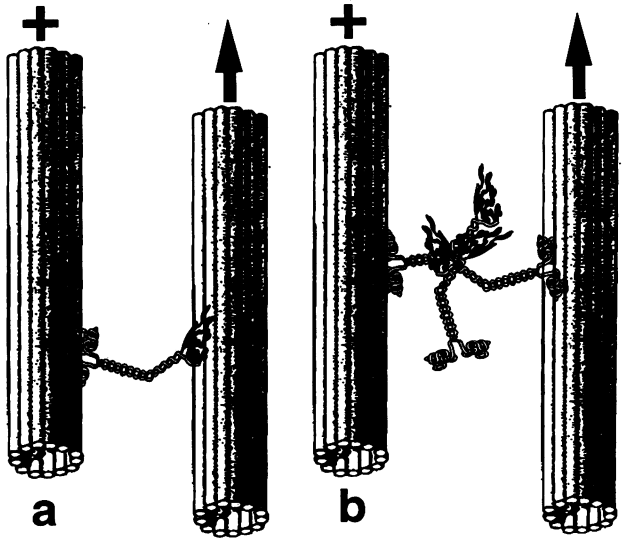

FIG. 5. Diagram showing alternate ways in which kinesin might form microtubule complexes. (*a*) Single kinesin bridge with its light- and heavy-chain ends attached to adjacent microtubules. (*b*) Oligomeric kinesin complex in which heavy chain ends provide attachments to microtubules. Drawings were adapted from Hirokawa *et al.* (4).

to find distorted kinesin crossbridges as well as sites where bridges appear to have been disrupted (Fig. 4 *d–f*). In some crossbridges, the kinesin, identified by its molecular mass, was substantially longer but still intact and bound to both microtubules (compare *b* and *d* in Fig. 4). These extended kinesins are similar to the previously reported structure of kinesins on highly attractive substrates (3, 4, 15, 24). They also appeared to be capable of sustaining tension since they remained attached, even when one of the microtubules had been split open (Fig. 4*d*). We also found a variety of sidearms that were not protofilaments; some of these may be fragments of kinesins still attached to one microtubule. These sidearms had a mean molecular mass of 228 ± 9 kDa (Table 1) and were characterized by stalks 20–25 nm long (Fig. 4*f*) or longer (Fig. 4*e*). The subunit composition of visible sidearms could not be unambiguously deduced from their structure, but it is evident that low molecular mass pieces derived from kinesin would not have been present if binding sites at either end of a bridging kinesin readily separated from the microtubule surface.

DISCUSSION

Purified microtubules become bundled into large, parallel arrays when they are mixed with kinesin and AMP-PNP. How kinesin mediates this bundling was initially puzzling because there was thought to be only one microtubule binding site on each heavy chain of the rod-shaped kinesin molecule. One plausible explanation for this bundling is that aggregates of kinesin molecules present multiple heavy-chain binding sites to microtubules (Fig. 5*b*). An alternative envisions crossbridging by single kinesin molecules, in which case a second microtubule binding site on the light-chain end of kinesin would seem to be required (Fig. 5*a*).

The present study distinguishes between the aggregate and the single kinesin models by directly imaging the crosslinked microtubule arrays and characterizing the crosslinking elements in low-dose, dark-field electron micrographs recorded with a field-emission STEM. Dark-field STEM images produce mass maps in which kinesins can be definitively identified by their molecular mass distribution and shape. Thus, single squid brain kinesin molecules have a molecular mass

of 379 ± 15 kDa, which is comparable to, but slightly heavier than, the mass predicted from sequence information—namely, 349 kDa (ref. 9; S. Beushausen, personal communication). Squid kinesins loosely adsorbed to carbon films are typically dumbbell-shaped and 40–52 nm long, which is notably shorter than that reported for kinesin from other sources (3, 4, 15, 24); this presumably reflects the degree to which the flexible kinesin molecule is adsorbed to, and unfolded by, the underlying support. The important question of how the different conformations of kinesin relate to its molecular organization and function remains unresolved, but we emphasize that this does not affect the identification of kinesins in microtubule–kinesin complexes.

Kinesins in microtubule bundles are difficult to recognize by STEM because they are low in mass relative to the microtubules and almost always overlap the edges of the microtubule to some extent. Nevertheless, favorably oriented crossbridges were found with sufficient frequency to conclude that their total molecular mass (360 ± 15 kDa) and shape (rods >25 nm long) are only consistent with single, complete kinesin molecules. The crosslinked arrays typically have an edge-to-edge spacing between microtubules of 25–35 nm, with a minimum of ≈25 nm. This spacing is consistent with a 40-nm length for a single kinesin, if one considers that the microtubule binding sites are near the ends of the molecule and that, as noted above, the ends often overlap the microtubule. The experiments on mechanically disrupted arrays indicate that the microtubule binding sites on both ends of the kinesin must be robust because both ends of the kinesin often remained attached, even while the stalk of the molecule was broken or the bridged microtubule unraveled.

A 25- to 35-nm spacing between microtubules, characteristic of kinesin-bundled microtubules, is not frequently observed in neurons (ref. 25, but see ref. 26). Indeed, the paucity of such close spacings has been interpreted to indicate that microtubules in axons are, by and large, not directly crosslinked (25). However, there are specific locations—such as the axon hillock in neurons and the mitotic spindle in dividing cells—where microtubules are consistently arranged in closely spaced, dense networks. Our observations suggest two possible roles for nonorganelle kinesin in such locations: directionally oriented motors to power microtubule sliding along other microtubules, thereby promoting extension of microtubule networks; or dynamic spacers, maintaining and tensioning the microtubule network in coordination with other cytoskeletal components. The latter function is illustrated by the finding that kinesin and dynein align endoplasmic reticulum along microtubules by opposing motor activities (27).

An appropriate opposition of kinesin-based forces might serve for dynamic stabilization in parallel microtubule arrays. In the axon, for instance, where microtubules have a plus end distal polarity, kinesins deployed with mixed orientations along a microtubule pair would pull in opposing directions. In general, kinesins randomly oriented on parallel microtubules with the same polarity would generate opposing forces, resulting in attachment and tensioning, but no net movement. Such forces might stabilize microtubule arrays but would not produce the telescoping movements that depend on one microtubule sliding along another. To produce sliding of parallel microtubules, the motors would have to attach to only one specific member of a microtubule pair, as is thought to occur for ciliary dynein.

Several recent studies on mitosis provide evidence that various kinesin-like proteins may act as motors to produce microtubule–microtubule sliding (28–30). Where microtubules are arranged *antiparallel* with overlapping plus ends, as in mitotic spindles, activation of a plus-end-directed motor would lead to spindle elongation. In the presence of the kinesin-like mitotic protein MKLP-1, antiparallel microtubules assembled *in vitro* bundle and slide over one another (28). This demonstration of kinesin-mediated microtubule sliding, as well as the ability of an antibody to this kinesin-like protein to block mitosis, suggests that such a mechanism may be responsible for spindle elongation. Studies on the assembly of mitotic spindles in *Saccharomyces cerevisiae* similarly indicate that kinesin-like proteins may be involved in generating forces or producing movement during mitosis (29, 30).

It thus appears that kinesins are capable of producing movement as well as stabilization within microtubule arrays. Which effect occurs may depend on the polarity of the microtubules and how the kinesins crosslinking a pair of microtubules are oriented. With regard to microtubule–microtubule sliding, the present results show that such movements could be mediated by organized arrays of kinesin molecules if the microtubules are arranged in antiparallel fashion, as they are in the dendrites of neurons and in developing axons (31).

We thank John Hunt for development of the digital STEM imaging system; Ruth Bechtold, Maureen O'Connell, and John Chludzinski for excellent technical assistance; and Frank Booy and Alasdair Steven for invaluable advice. Taxol was obtained courtesy of the Drug Synthesis and Chemistry Branch, National Cancer Institute.

1. Goldstein, L. S. B. (1991) *Trends Cell Biol.* **1**, 93–98.
2. Vale, R. D., Reese, T. S. & Sheetz, M. P. (1985) *Cell* **42**, 39–50.
3. Scholey, J. M., Heuser, J., Yang, J. T. & Goldstein, L. S. B. (1989) *Nature (London)* **338**, 355–357.
4. Hirokawa, N., Pfister, K. K., Yorifuji, H., Wagner, M. C., Brady, S. T. & Bloom, G. S. (1989) *Cell* **56**, 867–878.
5. Yang, J. T., Laymon, R. A. & Goldstein, L. S. B. (1989) *Cell* **56**, 879–889.
6. Yang, J. T., Saxton, W. M., Stewart, R. J., Raff, E. C. & Goldstein, L. S. B. (1990) *Science* **249**, 42–47.
7. Bloom, G. S., Wagner, M. C., Pfister, K. K. & Brady, S. T. (1988) *Biochemistry* **27**, 3409–3416.
8. Rodionov, V. I., Gyoeva, F. K., Kashina, A. S., Kuznetsov, S. A. & Gelfand, V. I. (1990) *J. Biol. Chem.* **265**, 5702–5707.
9. Kosik, K. S., Orecchia, L. D., Schnapp, B. J., Inouye, H. & Neve, R. L. (1990) *J. Biol. Chem.* **265**, 3278–3283.
10. Schroer, T. A. & Sheetz, M. P. (1991) *Annu. Rev. Physiol.* **53**, 629–652.
11. Brady, S. T., Pfister, K. K. & Bloom, G. S. (1990) *Proc. Natl. Acad. Sci. USA* **87**, 1061–1065.
12. Schnapp, B. J., Reese, T. S. & Bechtold, R. (1992) *J. Cell Biol.* **119**, 389–399.
13. Urrutia, R., McNiven, M. A., Albanesi, J. P., Murphy, D. B. & Kachar, B. (1991) *Proc. Natl. Acad. Sci. USA* **88**, 6701–6705.
14. Navone, F., Niclas, J., Hom-Booher, N., Sparks, L., Bernstein, H. D., McCaffrey, G. & Vale, R. D. (1992) *J. Cell Biol.* **117**, 1263–1275.
15. Hisanaga, S., Murofushi, H., Okuhara, K., Sato, R., Masuda, Y., Sakai, H. & Hirokawa, N. (1989) *Cell Motil. Cytoskeleton* **12**, 264–272.
16. Mandelkow, E.-M., Rapp, R. & Mandelkow, E. (1986) *J. Microsc.* **141**, 361–373.
17. Andrews, S. B., Leapman, R. D., Gallant, P. E. & Reese, T. S. (1991) in *Proceedings of the 49th Annual Meeting of Electron Microscopy Society of America*, eds. Bailey, G. W. & Hall, E. L. (San Francisco Press, San Francisco), pp. 152–153.
18. Dubochet, J., Adrian, M., Chang, J. J., Homo, J. C., Lepault, J., McDowall, A. W. & Schultz, P. (1988) *Q. Rev. Biophys.* **21**, 129–228.
19. Wall, J. S. & Hainfeld, J. F. (1986) *Annu. Rev. Biophys. Biophys. Chem.* **15**, 355–376.
20. Vale, R. D., Schnapp, B. J., Mitchison, T. J., Steuer, E., Reese, T. S. & Sheetz, M. P. (1985) *Cell* **43**, 623–632.
21. Leapman, R. D. & Andrews, S. B. (1992) *J. Microsc.* **165**, 225–238.
22. Johnson, K. & Wall, J. S. (1983) *J. Cell Biol.* **96**, 669–678.
23. Heuser, J. (1989) *J. Electron Microsc. Tech.* **13**, 244–263.
24. Amos, L. A. (1987) *J. Cell Sci.* **87**, 105–111.
25. Price, R. L., Lasek, R. J. & Katz, M. J. (1991) *Brain Res.* **540**, 209–216.
26. Chen, J., Kanai, Y., Cowan, N. J. & Hirokawa, N. (1992) *Nature (London)* **360**, 674–677.
27. Dabora, S. L. & Sheetz, M. P. (1988) *Cell* **54**, 27–35.
28. Nislow, C., Lombillo, V. A., Kuriyama, R. & McIntosh, J. R. (1992) *Nature (London)* **359**, 543–547.
29. Roof, D. M., Meluh, P. B. & Rose, M. D. (1992) *J. Cell Biol.* **118**, 95–108.
30. Saunders, W. S. & Hoyt, M. A. (1992) *Cell* **70**, 451–458.
31. Baas, P. W., Deitch, J. S., Black, M. M. & Banker, G. A. (1988) *Proc. Natl. Acad. Sci. USA* **85**, 8335–8339.